Vol. 39 (2008) *ACTA PHYSICA POLONICA B* No 5

CELLULAR AUTOMATA MODEL OF CARDIAC PACEMAKER*

Danuta Makowiec

Institute of Theoretical Physics and Astrophysics, Gdańsk University
Wita Stwosza 57, 80-952 Gdańsk, Poland

(Received January 5, 2008)

A network of Greenberg–Hasting cellular automata with cyclic intrinsic dynamics $F \rightarrow R \rightarrow A \rightarrow F \rightarrow \ldots$ is shown to be a reliable approximation to the cardiac pacemaker. The three possible cell's states F, R, A are characterized by fixed timings $\{n_F, n_R, n_A\}$ — time steps spent in each state. Dynamical properties of a simple line network are found to be critical with respect to the relation between n_F and n_R. The properties of a network arisen from a square lattice where some edges are rewired (locally and with the preference to link to cells which are more connected to other cells) are also studied. The resulted system evolves rhythmically with the period determined by timings. The emergence of a small group of neighboring automata where the whole system activity initiates is observed. The dominant evolution is accompanied with other rhythms, characterized by longer periods.

PACS numbers: 87.19.Hh, 87.17.Aa, 87.18.Mp

1. Introduction

The cells which constitute the cardiac muscle tissue have special properties which allow to consider the cardiac tissue to be the excitable medium, *i.e.*, the medium which have the ability to propagate signals without damping. The regular impulses, that result in rhythmic contractions of the heart, begin at the cardiac pacemaker called the sinoatrial node (SA node) [1]. The activity of the SA node spreads throughout the atria causing the atrial contraction. The same time this activity is passed to the atrioventricular node. Specialized conduction pathways: bundle of His and Purkinje fibers conduct the impulse throughout the ventricles causing the ventricle's contraction in an unison way.

---

[*] Presented at the XX Marian Smoluchowski Symposium on Statistical Physics, Zakopane, Poland, September 22–27, 2007.

Cellular automata are known to model the conduction properties in the excitable medium very well [2–4]. The simplest cellular automata system which can be used to model the excitable medium is known as Greenberg–Hastings model (GH model) [3]. The individual units — cells, with the simple three-state automaton's state space, are located in vertices of some regular lattice. An automaton changes its state because of the two reasons: the intrinsic state change rule or due to interactions with its nearest neighbors. The basic question posed in the GH model is the self-organization of the states of all automata to form the sustained characteristic spiral spatiotemporal patterns. It has been found that on the square lattice with the von Neumann neighborhood (the von Neumann neighborhood consists of the four cells which surround a central cell on a two-dimensional square lattice) there exist patterns which are persistent.

The GH model is being developed in two basic directions. The first direction is aimed on modeling, as close as possible, the activity of the heart tissue [5, 6]. Within this approach it has been demonstrated that the bursting rhythms are related to a single cell activity. Regular patterns of the spiral waves of activity were observed on a square lattice with the Moore (the Moore neighborhood consists of the eight cells that surround a central cell on a two-dimensional square lattice) or larger than the Moore neighborhoods.

The second direction in the GH model exploration is aimed on mathematical properties of the dynamical discrete system. Within this study, one considers, *e.g.* the self-organization in the cyclic cellular automata to model chemical reactions [7, 8].

In the following presentation, after short introduction to the physiology of the pacemaker, Sec. 2.1, we propose a cellular automaton, called by us FRA-CA, with the intrinsic dynamics of the GH-type but which additionally realizes the unique ability of the pacemaker cell, namely, the self-activation, Sec. 2.2. Then we investigate self-organization to the time limit states in the systems of interacting FRA-CA. In Sec. 3, two interacting FRA-CA are studied thoroughly. The three types of possible limit solutions are found and the conditions which lead to each limit solution are analytically proven. Then, dynamical properties in a line of FRA-CA with open boundary are examined. To speed up obtaining results we use the Monte Carlo simulations, Sec. 4.1. Finally, in Sec. 4.2, we present properties of a complex network of FRA-CA. By Monte Carlo methods we investigate how different timings of the intrinsic dynamics influence the periodicity in the stationary states of the network of FRA-CA, where the network structure is prepared in a way to be physiologically justified. We are specially interested in the problem of the emergence of diffusive patterns which are driven by the activity of a small group of FRA-CA.

2. FRA-CA model

2.1. Elements of pacemaker physiology

Each cell of a body is protected from the outside world by the membrane [1]. Many sophisticated mechanisms are built-in in the membrane to maintain the main membrane's role — the communication with the outside world. The different concentrations of ions between the inside and outside cell membrane are crucial for the electric potential across the membrane, called *the resting potential*. In the case of the excitable cells, *i.e.* myocytes — cells building the cardiac tissue, or neurons, the communication is related to changes in the membrane potential. The rapid increase in the membrane electrical potential, called *the action potential*, see Fig. 1, starts a sequence of changes in the activity of the membrane ion channels. The most important currents are currents of sodium Na^+, potassium K^+, and calcium Ca^{2+}.

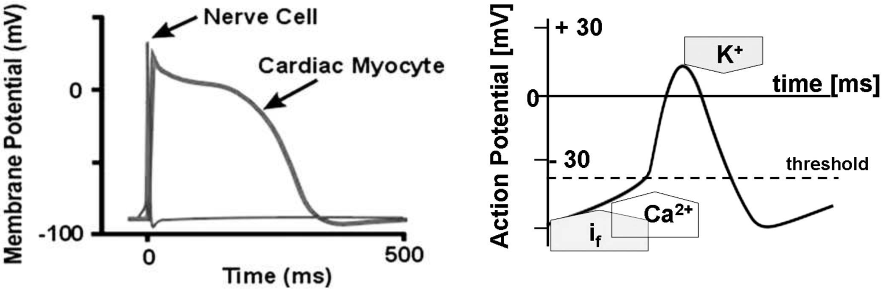

Fig. 1. Left panel: The activity of nerve and ventricle cells in time. Right panel: A cycle of intrinsic activity of a SA nodal cell. Arrows indicates at activity of ion currents. Both schema adapted from [1], color on-line.

The resting potential for a ventricular myocyte is about −90 mV. An external stimulus of the proper value can cause the sharp depolarization of the cell membrane. The sharp depolarization is due to the Na^+ currents while the Ca^{2+} currents extend the time duration of the high polarization of the membrane and delay the repolarization processes. During the repolarization phase the membrane potential is driven to restore of the resting potential.

The pacemaker cells are distinguished from other myocytes because their membranes do not posses the true resting potential but instead the membrane potential is slowly and spontaneously depolarized. The processes involved in the self-initiation are still discussed. It is known that so-called the funny current (i_{f} in Fig. 1) is one among mechanisms which slowly depolarizes a cell membrane. After reaching the threshold value the self-initiation to the new action potential takes place. Since the currents of Na^+ are not present here, then the fast depolarization process is not as rapid as in other myocytes. During the fast depolarization and repolarization processes, the cell is refractory to other stimuli. One can say that the membrane of any isolated pacemaker cell performs automatically a cyclic evolution. The state of the membrane switches subsequently from the slow depolarization processes by self-excitation to fast depolarization processes and then, through repolarization mechanisms, the cell membrane goes back to the starting point where the slow depolarization starts over again.

Most of the cardiac myocytes are elongated cells, see Fig. 2. Each cardiac cell contacts several other cells at specialized regions called *intercalated discs*. At these intercalated disks the cell membranes of two adjacent cells are extensively inter wound and bound together forming the so-called gap junctions. The intercalated discs are known to be low-resistant gap junctions between cells which form a functional syncytium. When one cell depolarizes, depolarizing current passes through gap junctions and depolarizes adjacent cells, what results in the cell-to-cell propagation of the action potential. One can say that interactions between cells are restricted to the network connections only.

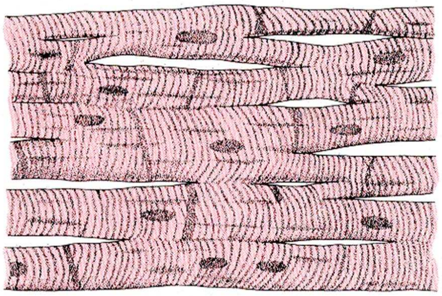

Fig. 2. A diagram showing the complex packing of myocytes in ventricular tissue, adapted from [9], color on-line.

In the SA node, inter cellular connections occur almost exclusively at small and simple intercalated disks located at various points along the sinus node myocytes. The analysis of the canine sinus node shows that typical SA nodal myocyte is connected to about of only 4.8 neighbors while a ventricle myocyte is connected to 11.3 cells on average. Moreover, about 3.5 neighbors of SA nodal cells are connected lateral, *i.e.* differently from end-to-end or side-to-side orientations [11].

It is known that the action potential, which then leads to the contraction of the whole heart, is initiated in a small part of the SA node called *the leading pacemaker*. The leading pacemaker is usually located in the center of the SA node. But it is known that the leading pacemaker site can be shifted from the center toward the periphery. It could happen, for example, in response to the autonomic nerve stimulation [12]. The activation of the leading pacemaker propagates to the periphery of the SA node which is called *the crista terminalis* and then onto the atrial muscle.

Cellular automata are dynamical systems which are perfectly discrete, *i.e.* the space, states and time are discrete. The three stages of the individual SA nodal cell activity are well suited to be coded into a three state cellular automaton. Moreover, the cell-to-cell activity transmission can be directly represented by the cellular automata local rule of interactions. Since the space distribution of cells can be considered as flat and regular, the square lattice approach is a good starting point.

2.2. FRA-CA definition

The space of a GH automaton Σ consists of three elements denoted F, R, A which correspond to the three main activities of the cell membrane: F — *firing* — fast depolarization, R — *resting* — repolarization to recover the resting potential and A — *activity* — awaiting for a next stimulus. Automata are placed on a regular d dimensional lattice Z^d. The following dynamics is considered:
— for $\sigma_i(t) \in \{F, R, A\}$ and N_i set of neighbors of an ith lattice vertex:

$$\sigma_i(t+1) = \begin{cases} R & \text{if} \quad \sigma_i(t) = F\,, \\ A & \text{if} \quad \sigma_i(t) = R\,, \\ F & \text{if} \quad \sigma_i(t) = A \text{ and } \sigma_j(t) = F \text{ for some } j \in N_i\,, \\ A & \text{otherwise}\,. \end{cases} \tag{1}$$

To incorporate the property that an automaton stays in one of the three states: F, R, A for the fixed numbers of time steps n_F, n_R, n_A let the state space be represented as $\Sigma^* = \left\{ \binom{F}{f}_{1,\ldots,n_F}, \binom{R}{r}_{1,\ldots,n_R}, \binom{A}{a}_{1,\ldots,n_A} \right\}$ where F, R, $A \in \Sigma$ and $1 \le f \le n_F$, $1 \le r \le n_R$, $1 \le a \le n_A$ count the number of time steps spent by an automaton in the corresponding state.
Let *next* : $\{F, R, A\} \to \{F, R, A\}$ denote the following permutation $\begin{pmatrix} F & R & A \\ R & A & F \end{pmatrix}$.
If at a time step t the state of an automaton is $\binom{\sigma}{s}$ where $1 \le s \le n_\sigma$ and $n_\sigma \in \{n_F, n_R, n_A\}$ is determined by σ, then, due to *the intrinsic rule*, the next state of the automaton is:

$$\binom{\sigma}{s}(t) \overset{t \to t+1}{\longmapsto} \begin{cases} \binom{\text{next}(\sigma)}{1} & \text{if } s = n_S\,, \\ \binom{\sigma}{s+1} & \text{otherwise}\,. \end{cases} \tag{2}$$

The intrinsic transition rule establishes the periodic dynamics with the period length $T = n_F + n_R + n_A$. We will call just introduced automaton the FRA cellular automaton (FRA-CA). *The phase* $\phi : N \to \{0, 1, \ldots, T-1\}$ of a intrinsic cycle of FRA-CA is described as follows:

$$\begin{array}{lll} \phi(t) & = 0 \quad \Leftrightarrow & \binom{\sigma}{s}(t) = \binom{F}{1}\,, \\ \phi(t+1) & = \phi(t) + 1 & \quad \text{otherwise}\,. \end{array} \tag{3}$$

3. Two interacting FRA-CA

Consider the two FRA-CA named **A** and **B** with the intrinsic dynamics characterized by the same timings: n_F, n_R, n_A. The state of each automaton can be described by its phase: ϕ_A and ϕ_B, suitable. Let $\Delta(t) = \phi_A(t) - \phi_B(t)$ denote the phase difference between the two automata at time t. Notice that, if the phase difference between two FRA-CA: **A** and **B**, is 0 then no change in the phase difference can be observed, *i.e.*:

$$\Delta(t) = 0 \quad \Rightarrow \qquad \forall_{t'>t} \Delta(t') = 0\,.$$

Let an *active* automaton start to be *firing* in the next time step if the other automaton is in *firing* at present. We say one automaton is impacted by the other one.

It appears that in a system of two FRA-CA only the following limit evolutions can arise:

- *The rules adjusted evolution* — if the results of both rules: intrinsic and interactions between the automata are the same.
- *The alternating impacts evolution* — if within each period two events of impacts take place. The first event means **A** automaton is impacted by **B** automaton — **A** automaton is switched to *firing*. Then the second event occurs — **B** automaton is impacted by **A** automaton what switches **B** automaton to *firing*.
- *The quiet evolution* — there are not any impacts between the automata.

Remark: Both stabilizations: the rules adjusted evolution and quiet evolution, establish the periodic system with the period equal to $T = n_F + n_R + n_A$ while the alternating impacts evolution provides the periodic system with the period equal to $T^* = n_F + n_R + 1$. The period T^* is the minimal period which can arise in the system of two FRA-CA.

It appears that which of the limit evolution is reached — rules adjusted evolution, alternating impacts evolution or quiet evolution, depends on the difference between initial phases of the automata:
let t be the moment when one of the two automata, **A**, switches to *firing* as the first automaton of the pair:

case $n_R < n_F$**:**

$\diamond$ if the state of the second automaton is $\binom{R}{1}$ then the system evolves the alternating impacts evolution, since the following sequence of state take place:

$$\begin{array}{lllllllllll}
\text{time} & t & & \star\downarrow & & & & & & & \star\uparrow \\
\mathbf{A}: & \binom{F}{1} & \cdots\cdots\cdots & \binom{F}{f} & \binom{F}{f+1} & \cdots & \binom{F}{n_F} & \binom{R}{1} & \cdots & \binom{R}{n_R} & \binom{A}{1}, \\
\mathbf{B}: & \binom{R}{1} & \cdots\binom{R}{n_R} & \binom{A}{1} & \binom{F}{1} & \cdots\cdots\cdots & \cdots\cdots & \cdots & & & \binom{F}{n_F},
\end{array}$$

where $\star\downarrow$ ($\star\uparrow$) denotes the moment of time when **A** (**B**) automaton is impacted by **B** (**A**) automaton. We see that within $n_F + n_R + 1$ steps the system is back to the initial situation due to the two impacts. At first **B** automaton is impacted by **B** automaton then **A** automaton is impacted by **A** automaton.

$\diamond$ if the state of the second automaton is $\binom{F}{f}$ and if $f > n_R + 1$ then the system evolves the alternating impacts evolution; if $f \leq n_R + 1$ then the system arrives to the rules adjusted evolution. To see this fact let us consider subsequently: $f = n_R + 2$

$$\begin{array}{llllllll}
\text{time} & & & & \star\downarrow & & & \star\uparrow \\
\mathbf{A}: & \binom{F}{1} & \cdots\cdots\cdots & \cdots\cdots\cdots & \binom{F}{n_F} & \binom{R}{1} & \cdots & \binom{R}{n_R}\binom{A}{1}, \\
\mathbf{B}: & \binom{F}{f} & \cdots\binom{F}{n_F} & \binom{R}{1}\cdots\binom{R}{n_R} & \binom{A}{1} & \binom{F}{1} & \cdots\cdots & \binom{F}{f'-1},
\end{array}$$

what denotes that $n_F + n_R + 2 = n_F - f + 1 + n_R + 1 + f'$ so $f = f'$ and after $n_R + n_F + 1$ steps the system is back in the initial state.

$f > n_R + 2$

$$\begin{array}{lllllllll}
\text{time} & & & & \star\downarrow & & & & \star\uparrow \\
\mathbf{A}: & \binom{F}{1} & \cdots\cdots\cdots & \cdots\cdots\cdots & \binom{F}{f'-1} & \binom{F}{f'} & \cdots\binom{F}{n_F} & \binom{R}{1}\cdots & \binom{R}{n_R}\binom{A}{1}, \\
\mathbf{B}: & \binom{F}{f} & \cdots\binom{F}{n_F} & \binom{R}{1}\cdots\binom{R}{n_R} & \binom{A}{1} & \binom{F}{1} & \cdots\cdots\cdots & \cdots\cdots\cdots & \binom{F}{f''-1}.
\end{array}$$

Since $f' = 2 + n_R + n_F + 1 - f$ then $f'' = n_F + n_R + 3 - f' = f$ what denotes that the system follows the alternating impacts evolution.

if $f \leq n_R + 1$ then $n_F \leq n_R + n_F - f + 1$ what means that the interval when **B** is in the *resting* state extends beyond **A** automaton is being in $\binom{F}{n_F}$. Then one of the two situations takes place:

[a] $n_F - f + 1 + n_R + n_A > n_F + n_R \quad \Leftrightarrow \quad f < n_A + 1$
what means that the following evolution takes place:

$$\begin{array}{l}
\text{time} \hfill \star\uparrow \\
\mathbf{A}: \binom{F}{1} \qquad \cdots\cdots\cdots\cdots \binom{F}{n_F}\binom{R}{1} \cdots\cdots\cdots\cdots \binom{R}{n_R}\binom{A}{1} \cdots\cdots \binom{A}{a}, \\
\mathbf{B}: \binom{F}{f}\cdots\binom{F}{n_F}\binom{R}{1} \cdots\cdots\cdots\cdots \binom{R}{n_R}\binom{A}{1} \cdots\cdots\cdots\cdots \binom{A}{n_A}\binom{F}{1}.
\end{array}$$

Hence after $n_F - f + 1 + n_R + n_A = T - f + 1$ steps **AB** automaton is impacted by **A** automaton. With the roles of **A** and **B** exchanged the system is in the situation considered earlier. Therefore, in the next time step the rules adjusted evolution starts.

[b] $n_F - f + 1 + n_R + n_A \leq n_F + n_R \quad \Leftrightarrow \quad f \geq n_A + 1$
which takes place if $n_A < n_F$ and $n_A < n_R$. Then changes in the system are the following:

$$\begin{array}{l}
\text{time} \hfill \star\uparrow \\
\mathbf{A}: \binom{F}{1} \qquad \cdots\cdots\cdots\cdots \binom{F}{n_F}\binom{R}{1} \cdots\cdots\cdots\cdots\cdots\cdots\cdots\cdots\cdots\cdots \binom{R}{n_R}\binom{A}{1}, \\
\mathbf{B}: \binom{F}{f}\cdots\binom{F}{n_F}\binom{R}{1} \cdots\cdots\cdots\cdots \binom{R}{n_R}\binom{A}{1}\cdots\binom{A}{n_A}\binom{F}{1}\cdots\binom{F}{f'-1}.
\end{array}$$

Here after $n_F + n_R + 1$ steps **AB** automaton is impacted by **B** automaton. In the next time step **A** is in $\binom{F}{1}$ and **B** is in $\binom{F}{f'}$ with $f' = f - n_A + 1$. The system is back in the initial state but with the phase difference between automata shortened by $n_A - 1$. If $f' < n_A + 1$ then the system evolves like that one considered in the [a] case. If $f' \geq n_A + 1$ then the next impact **B** on **A** makes again the reduction of the phase difference. After $k = 1, 2, \ldots$ times of the above described reduction, where $k = \max'_k\{f - k'(n_A - 1) > 0\}$, *i.e.* at $t = k(n_F + n_R + 1)$ the system arrives at the evolution described in the [a] case. Thus the both cases lead to the rules adjusted evolution.

$\diamond$ if the state of the second automaton **B** is $\binom{R}{r}$ and $r > 1$ then the rules adjusted evolution emerges. This property arises directly from the following sequence of events:

$$\begin{array}{l}
\text{time } t \hfill \star\downarrow \qquad\qquad \\
\mathbf{A}: \binom{F}{1} \cdots\cdots\cdots \binom{F}{f-1}\ \binom{F}{f}, \\
\mathbf{B}: \binom{R}{r}\cdots\binom{R}{n_R}\ \binom{A}{1}\ \ \binom{F}{1},
\end{array}$$

where $f = (n_R+1)+(2-r)$. For $r > 1$ it means that $f \leq n_R+1$ what by our earlier results mean that evolution settles as the rules adjusted evolution.

case $n_R \geq n_F$**:**

if the state of the second automaton at t is $\binom{R}{r}$ where $n_A + 1 \leq r \leq n_R - n_F + 1$ then the system evolves the quiet evolution; otherwise the system arrives to the rules adjusted evolution:

If $r = 1$, then depending on n_A, the following two evolutions are possible: either

$$\begin{array}{ll}
\text{time } t & \hfill \star\uparrow \\
\mathbf{A}: & \binom{F}{1}\cdots\binom{F}{n_F}\binom{R}{1}\ \cdots\cdots\cdots\ \binom{R}{n_R}\binom{A}{1}\ \cdots\cdots\ \binom{A}{a}, \\
\mathbf{B}: & \binom{R}{1}\ \cdots\cdots\cdots\ \binom{R}{n_R}\binom{A}{1}\ \cdots\cdots\cdots\ \binom{A}{n_A}\binom{F}{1},
\end{array}$$

what leads to the rules adjusted evolution, or

$$\begin{array}{ll}
\text{time } t & \hfill \star\uparrow \\
\mathbf{A}: & \binom{F}{1}\cdots\binom{F}{n_F}\binom{R}{1}\ \cdots\cdots\cdots\cdots\cdots\cdots\ \binom{R}{n_R}\ \binom{A}{1}, \\
\mathbf{B}: & \binom{R}{1}\ \cdots\cdots\cdots\ \binom{R}{n_R}\binom{A}{1}\cdots\binom{A}{n_A}\binom{F}{1}\cdots\binom{F}{f-1},
\end{array}$$

where f value is determined the condition $f + n_A + n_R = n_F + n_R + 2$ what leads to the rules adjusted evolution.

Let $r > 1$. If $r > n_R - n_F + 1 \Leftrightarrow n_R - r + 1 < n_F$ then the following two Situations are possible:

$$\begin{array}{lcccccccccc}
\text{time} & & & \star\downarrow & & & & & \star\downarrow & & \\
\mathbf{A}: & \binom{F}{1} & \cdots\cdots & \binom{F}{f-1} & \binom{F}{f} & \text{or} & \binom{F}{1} & \cdots\cdots & \binom{F}{n_F} & \binom{R}{1}, \\
\mathbf{B}: & \binom{R}{r} & \cdots\binom{R}{n_R} & \binom{A}{1} & \binom{F}{1} & & \binom{R}{r} & \cdots\binom{R}{n_R} & \binom{A}{1} & \binom{F}{1}.
\end{array}$$

The both cases by our earlier considerations lead to the rules adjusted evolution.

If $n_R - r + 1 < n_F$ and $n_A + 1 > r \Leftrightarrow n_F + n_A + n_R - r + 1 < n_F + n_R$ then similar arguments prove the stabilization with the rules adjusted evolution.

If $n_A + 1 \leq r \leq n_R - n_F + 1$ then the evolution goes as follows:

$$\begin{array}{l}
\text{time} \\
\mathbf{A}: \\
\binom{F}{1}\cdots\binom{F}{n_F}\binom{R}{1}\cdots\cdots\cdots\cdots\cdots\cdots\cdots\cdots\cdots\binom{R}{n_R}\binom{A}{1}\cdots\binom{A}{n_A}\binom{F}{1}, \\
\mathbf{B}: \\
\binom{R}{r}\cdots\cdots\cdots\binom{R}{n_R}\binom{A}{1}\cdots\binom{A}{n_A}\binom{F}{1}\cdots\binom{F}{n_F}\binom{R}{1}\cdots\cdots\cdots\cdots\binom{R}{r'},
\end{array}$$

with r' determined by the condition $1+n_A+n_R+n_F = r'+n_R-r+1+n_A+n_F$ what denotes $r' = r$. The evolution develops without any interactions. Hence any initial phase difference is conserved — the evolution is quiet.

4. Monte Carlo studies of FRA-CA

By analytical investigations of the interactions between the two FRA-CA we have identified the three possible stable solutions: adjusting rules evolution, alternating impacts evolution and quiet evolution. We also have given all conditions which lead to each of the stable solutions.

One can see the alternating impacts solution as the maximally active dynamics since both cells from a pair intensively interact with each other. Because of the intensity of impacts the intrinsic periods of both automata are shortened to the shortest possible $T^* = n_F + n_R + 1$ and the whole system evolves with this period.

The other two solutions are also periodic but the period is equal to the intrinsic period of the FRA-CA, *i.e.* $T = n_F + n_R + n_A$. Since if $n_R > n_F$ only solutions with T occur, then for n_A typical only the rules adjusted evolution appears. Since the rule adjusted evolution is of the diffusive type — only one cell is impacted by the other one, it is interesting to ask if the phase adjustment occur if we consider interactions of many FRA-CA. The case of $n_R > n_F$ is physiologically interesting because it is known that the time used by a myocyte for a fast depolarization is shorter than the time spent on repolarization processes or during the slow depolarization [10].

The analytical method of investigations used in the previous section is exhausted. Therefore we are switching to the Monte Carlo approach. By random drawings of initial states of cellular automata, and then by including also a random choice of the network structure and stochastic changes in timings, we performed tests in the parameter space to extract typical behaviors of the studied systems.

4.1. A line of FRA-CA

Subsequently, by setting the values of n_F, n_R, n_A from 2 to 50 with a step equal to 1, we performed simulations of $N = 100$ FRA-CA arranged in a line. Each setting (n_F, n_R, n_A) was applied to a 100 different random initial states of FRA-CA. Within 20000 time steps the evolution of the most of FRA-CA stabilized but in the case when n_F was large ($n_F > 25$) and n_A ($n_A < 5$) was small then 80000 time steps had to be used to reach the stabilization.

We found all systems evolving exactly with one of the two periods: either $T = n_F+n_R+n_A$ or $T^* = n_F+n_R+1$. Depending on the model parameters the probability to find which of the two periods T or T^* occur was different.

In Fig. 3 we present the results which we received when $n_F = 25$. They are representative for other values of n_F in the sense that the transition appears when the resting time n_R crosses the firing time n_F:

— *if* $n_F \leq n_R$ *only the solution with the period* T *happens;*

— *if* $n_F > n_R$ *the solution with the period* T^* *is significantly more probable.*

One should notice the symmetry between the plots describing the probability of events with periods T and T^*. This symmetry reflects the fact that no other periods were observed.

When $n_F \leq n_R$, hence the final state is periodic with T, and if and n_A is large enough, so that the quiet evolution cannot emerge, then the phase adjustment between pairs of neighboring automata is present, see Fig. 3, the bottom figure. Thus the whole system evolves the rules adjusted evolution. We have to add that in all cases when we found the evolution periodic with the period length T when $n_F > n_R$ then the phase adjustment between all pairs was always found.

Searching among details of particular configurations of systems which evolve with period T^* we discovered that to establish the stabilization with T^*, it was enough that there existed a single pair which followed the alternating impacts evolution. The periodicity of that pair was then propagated to the both ends of a line because the rest of the automata pairs had phases adjusted. Such final configurations were received most frequently. However, we observed also such stable configurations where more pairs (*e.g.* a chain of pairs) with the alternating impact evolution were present. However, we did not notice any other mechanisms than a pair evolving alternating impacts evolution, which led to the stabilization with T^* period.

Therefore a line of FRA-CA can be thought as the first approximation to the real cardiac pacemaker. Depending on the relation between the timings n_F, n_R, n_A not only the length of beating of the pacemaker is changed but also the switch between two types of inter cells dynamics takes place. The first type dynamics can be interpreted as the active dynamics since it relies on a pair of neighboring automata which follows the alternating impacts evolution. The second type of the automata dynamics should be seen as the passive dynamics because of the overwhelming presence of pairs of automata between which the phases are adjusted. Such phase adjustment provides the system that is perfectly prepared to conduct signals. Appearance of both dynamics can be related to the known properties of the sinus node — presence of the leading cells which initiate the activity of the whole system, and which are surrounded by cells which though have the ability to self-generate the activity but they serve as the medium which transmit the leading cells activity to the outside SA node [12].

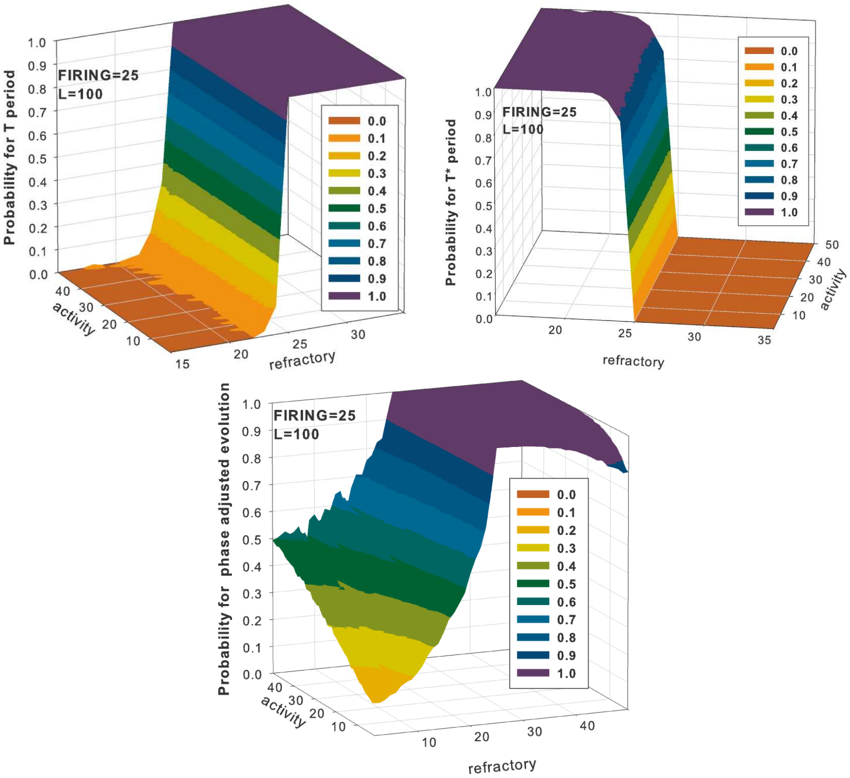

Fig. 3. The probability to find: stabilization with the period T (left) or T^* (right) and a pair with adjusted phases (bottom), is shown when $firing = 25$ for different activity and resting lengths. A line of $N = 100$ FRA-CA is considered, color on-line.

4.2. FRA-CA on a complex network

Let us start with a set of N FRA-CA located in vertices of the regular square lattice and $N = L \times L$. Basing on the physiologically known facts about the SA nodal cells arrangement, compare Sec. 2, let us consider the preference to askew connections and discard the vertical links, by the following procedure: for a given probability d: a vertical interaction is created with $d/2$ probability, an askew edge is created with d and a horizontal edge with $2d$ probability. To enhance the line structure let us work with $d = 0.45$.

Moreover, to make the structure of interactions uneven, let some of the described connections be stochastically rewired. The proposed rewiring procedure is local and with the preference set to the vertex degree. It goes as follows: see Fig. 4 left:

For a given p — *probability of rewiring* and p_{f} — *threshold for vertex degree preference*

- For a given automaton A when choosing a connection to rewire, an automaton less connected with others is preferred. The probability to unlink the A automaton from a vertex B is calculated as follows:

$$p_{\mathrm{unlink}} = p \quad \frac{p_{\mathrm{f}}}{\deg(B)}\,.$$

- To make the rewiring local, a new automaton B′ which will be linked to the automaton A is chosen only from the actual neighbors of B automaton. While searching among neighbors, the preference is set to the cells that are most densely connected to others. The probability to link A automaton to B′ automaton is calculated as follows:

$$p_{\mathrm{link\_to}} = \frac{\deg(B')}{p_{\mathrm{f}}}\,.$$

- To preserve the line structure, any horizontal connection is forbidden to be rewired.

In Fig. 4 on the right side we show the vertex degree distributions calculated for the networks resulted after applying the above algorithm with $p = 0.01$ and for different values of p_{f} a hundred Monte Carlo steps. Following results of that experiment we have found that $p_{\mathrm{f}} = 4$ describes best the canine SA node structure, compare Sec. 2.

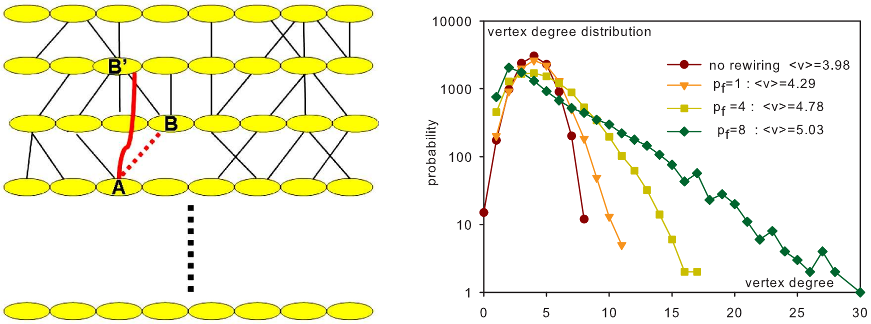

Fig. 4. Left: An illustration of the algorithm of rewiring. The connection between A and B is changed into the connection between A and B′. A red doted edge is rewired to a red solid edge. Right: A vertex degree distribution in the resulting networks: $L = 100$, $d = 0.45$, $p = 0.01$, the algorithm of rewiring is applied 100 MCS, color on-line.

The intrinsic dynamic rule (2) is deterministic what is closely related with the physiologically observed fact that the lengths of the fast depolarization and repolarization phases are strongly fixed. Hence any changes in timings n_F, n_R and n_A from a period to a period of our artificial FRA-CA should be rather limited. Therefore, let us consider the little probable possibility of shortening each of n_F, n_R and n_A value what effects that we introduce a nonzero probability to switch the actual automaton state to the next state in its internal cycle. We propose to perform the stochastic evolution as follows:

$$\binom{\sigma}{s}(t) \overset{t\to t+1}{\longmapsto} \begin{cases} \binom{\mathrm{next}(\sigma)}{1} & \text{with} \quad \text{probability} \quad (\frac{s}{n_S})^{\xi}\,, \\ \binom{\sigma}{s+1} & \text{with} \quad \text{probability} \quad 1-(\frac{s}{n_S})^{\xi}\,, \end{cases} \tag{4}$$

where if $\xi \gg 1$ then we restore the deterministic evolution. Notice that for $\xi > 1$ only very few last steps could be skipped and therefore the effective timings are closely determined by values of n_F, n_R and n_A.

Finally, let as assume that the threshold for firing an automaton equals to 1, *i.e.* at least two neighbors in the *firing* state are needed to switch an automaton from the state of *activity* to the *firing* state. But since the horizontal connections are known to be much larger and more efficient than others, we additionally assume that the influence of the horizontal connections is doubled. Hence only one left or right neighbor being in the *firing* state is able to activate the cell.

By Monte Carlo simulation we ask whether the resulting stationary evolution is periodic and what the period length is. We also investigate if the sharp transition tuned by n_R crossing n_F value and the switch between evolution with T and T^* period is still present.

The network state is measured by number of FRA-CA staying in the *firing* state in the most left column I_{left} and in the most right column I_{right}. These currents are assumed to imitate signals which arrive at the crista terminalis. Additionally, we also consider a total signal I_{total} which counts all cells which are in the *firing* state.

In Figs. 5, 6 and 7 the typical results are shown for various settings of timings n_F, n_R, n_A. We present pieces of time series corresponding to signals received from stationary states and their power spectra to identify periodicity. The presented figures are representative in the following sense. At all settings of n_F, n_R, n_A the networks of FRA-CA provide systems which exhibit periodicity with the basic period value about T^*. There are evident maxima in all plots of the power spectra though, because of the introduced stochasticity into intrinsic dynamics, these maxima in the power spectra plots are wide and moved to right. In Fig. 7 the example illustrating this statement is given. The two settings of n_F, n_R, n_A lead to the systems in

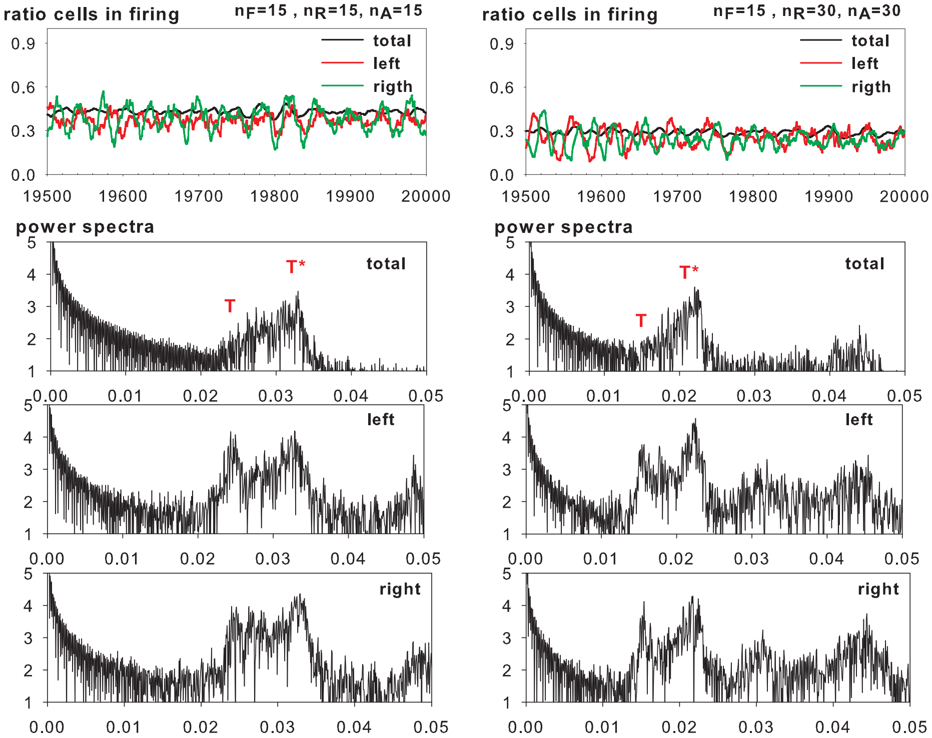

Fig. 5. Properties of stationary series of the described network with FRA-CA: the times series of $I_{\text{total}}, I_{\text{left}}, I_{\text{right}}$ and the their power spectra. By T and T^* the frequencies corresponding to these periods are shown. Left column $n_F = 15$, $n_R = 15, n_A = 15$ and right column $n_F = 15, n_R = 30, n_A = 30$, $L = 100$.

which T^* is identical but the intrinsic periods are distinct. Thus the critical transition in the dynamics related with n_F crossing n_R is not present. Both dynamics coexists in the systems. A dominant evolution is related with T^* period but there are present other oscillations with longer cycles also.

While the total signal I_{total} is usually rather regular and stable, the border signals: I_{left} and I_{right} vary significantly in time. Moreover the amplitudes of I_{left} and I_{right} oscillations are usually higher than the amplitude of I_{total} oscillations.

It appears that the stationary state configurations are organized in well developed spiral patterns, see Fig. 8. These patterns correspond to cells in the *firing* state. If T^* is comparable to the linear size of the network, L, then usually there is observed a single origin of the spiral pattern. In other cases there are many spiral-type patterns developed at the same time. In such cases one can observe clusters of the moving activity. We believe

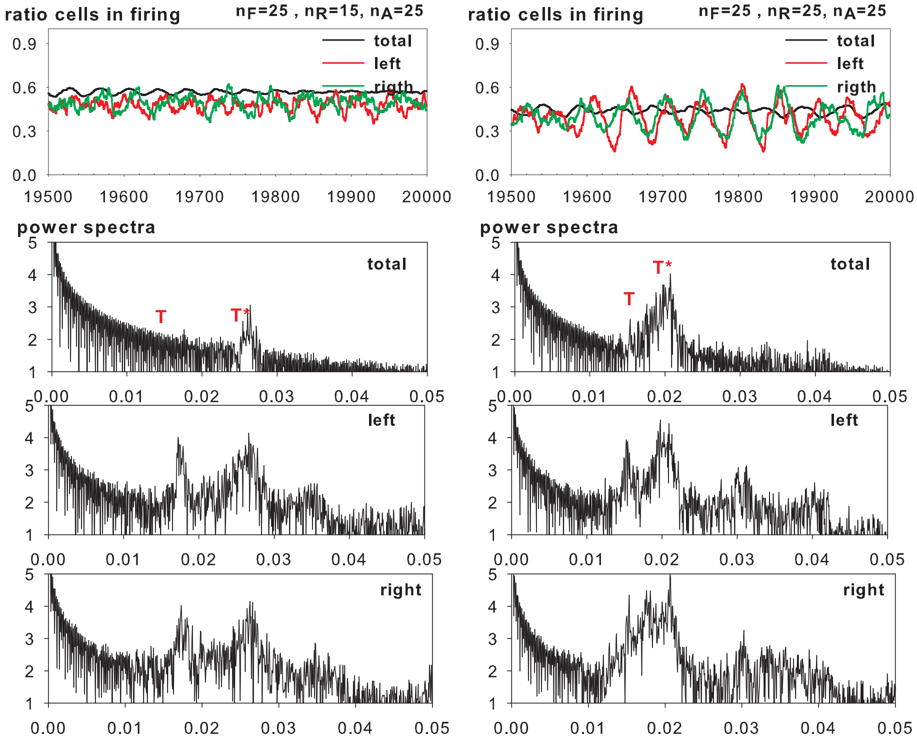

Fig. 6. Properties of stationary series of the described network with FRA-CA: the times series of $I_{\text{total}}, I_{\text{left}}, I_{\text{right}}$ and the their power spectra. By T and T^* the frequencies corresponding to these periods are shown. Left column $n_F = 25$, $n_R = 15, n_A = 25$ and right column $n_F = 25, n_R = 25, n_A = 25$, $L = 100$.

that emergence of such patterns is an indicator at the regions where the evolution relies on cells with adjusted phases, what denotes that the cells follow the passive dynamics. Moreover, we believe that in the centers of the spiral patterns there are few cells which are tightly joined together by the alternating impacts evolution. We observe that these sources of the spiral patterns are rather long living structures though a kind of a stochastic walk of these centers occurs. This walk is probably due to the stochasticity in the intrinsic dynamical rule. Moreover, one can also observe that new centers emerge and then a kind of a battle between centers takes place.

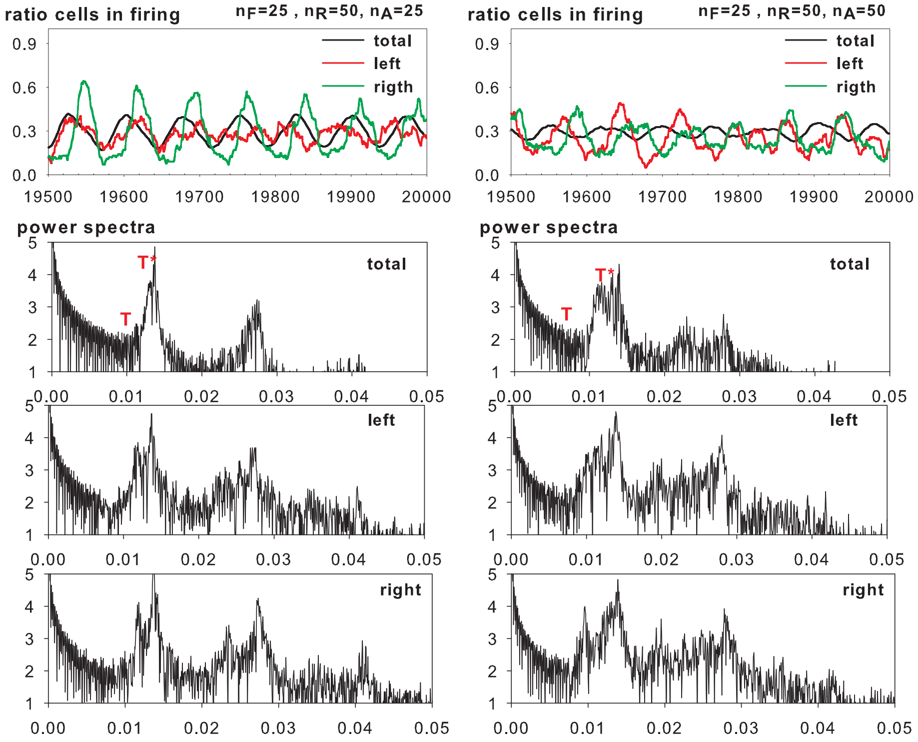

Fig. 7. Properties of stationary series of the described network with FRA-CA: the times series of $I_{\text{total}}, I_{\text{left}}, I_{\text{right}}$ and the their power spectra. By T and T^* the frequencies corresponding to these periods are shown. Left column $n_F = 25$, $n_R = 50, n_A = 25$ and right column $n_F = 25, n_R = 50, n_A = 50$, $L = 100$.

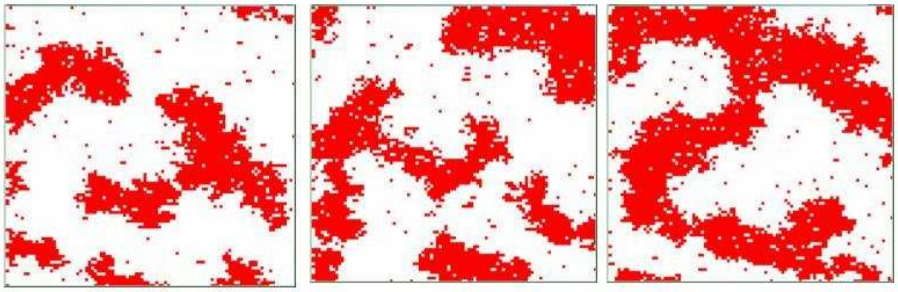

Fig. 8. Snapshots from the typical evolution of the FRA-CA system, case $n_F = 25$, $n_R = 65, n_A = 25$ and $L = 100$.

5. Conclusions

The theoretical studies of the two interacting FRA-CA have provided us strong insights on possible stable evolutions of multi-cell systems. We have identified two distinct types of solutions: (a) the active evolution which relies on the permanent interactions between automata and effects in the shortest possible oscillations of the total system and (b) the passive evolution which relies on the perfect adjustment between interactions and the intrinsic cyclic dynamics.

When considering systems consisting of many FRA-CA arranged in either a simple topology (a line structure) or in a complex one (diluted square lattice with local rewirings), we have been concentrated on the self-organization to the rhythmic evolution with the period driven by the active dynamics. We have found that in the case of the linear arrangement of FRA-CA there was a sharp transition between the two possible types of the evolutions. The transition was related to the difference between time steps needed for the repolarization n_R and times steps used for fast depolarization n_F. However, in the case of the complex networks the active oscillations were always present what could be concluded that the network topology was crucial for vanishing of the criticality in the network of FRA-CA.

We have found also that the active dynamics was driven by a small group of neighboring automata which followed the alternating impacts evolution. In the case of the complex topology, that property was concluded after investigations of spatio-temporal long living structures. Therefore we could think about the small group of cells which was the source of the active evolution that it was a fingerprint of emerging of the center with the leading cells. There was also noticed that, on the background of the dominant oscillations, some other (with longer periods) oscillations were present.

The model in our simulations considers 10 000 cells. In the case of humans it is known that the SA node consists of about 70 000 cells [1]. Hence to obtain on-to-one mapping we should increase the size of considered system. Our future work will go in this direction. Moreover, since it is known that the SA nodal cells are not identical and that differences between cells are systematic — the further from the center of the sinus node the cell is then the difference between center cell and periphery cell is more evident, then when enlarging the system, we will take into account this physiological observation.

The three-state state space of the automaton, used by us, is definitely over simplification to take the problem of the variety of the possible cells. Moreover, the myocytes are surrounded by the connective tissue matrix and microvessels. All together form an anisotropic cellular network which structure is not fully understood. Hence the network construction proposed here seems to be too rough.

The presented investigations are only preliminary and are not claimed to be completed. However, we hope that by comparing the physiologically known properties and our results we provide hints on the cellular network of the SA node.

This work is supported by the University of Gdańsk, BW-5400-5-0090-8.

REFERENCES

[1] R.E. Klabunde, Cardiovascular Physiology Concepts, 2007, `http://www.cvphysiology.com`

[2] G.B. Ermentrout, L. Edelstein-Keshet, *J. Theor. Biol.* **160**, 97 (1993).

[3] J.M. Greenberg, S.P. Hastings, *SIAM J. Appl. Math.* **34**, 515 (1978).

[4] M. Markus, B. Hess, *Nature* **347**, 56 (1990).

[5] G. Bub, L. Glass, N.G. Publicover, A. Shrier, *Proc. Natl. Acad. Sci. USA* **95**, 10283 (2005).

[6] G. Bub, A. Shrier, L. Glass, *Phys. Rev. Lett.* **94**, 028105 (2005).

[7] D. Griffeath, R. Durrett, *J. Exp. Math.* **2**, 183 (1993).

[8] J.M. Greenberg, C. Greene, S.P. Hastings, *Int. J. Unconventional Comput.* **1**, 399 (2005).

[9] R.A. Luke, J.E. Saffitz, *J. Clin. Invest.* **87**, 1594 (1991).

[10] I. Kodama, H. Honyo, M.R. Boyett, *J. Cardiovasc. Electrophysiol.* **13**, 1303 (2002).

[11] J.E. Saffitz, D.L. Lerner, K.A. Yamada, *Gap Junctions Distribution and Regulation in the Heart* in *Cardiac Elecrophysiology. From Cell to Bedside*, D.P. Zipes, J. Jalive eds., Saunders Co., Philadelphia, PA USA 2004, p. 181.

[12] I. Kodama, H. Honyo, H. Dobrzynski, M.R. Boyett, *Cellular Mechanisms of Sinoatrial Activity* in *Cardiac Elecrophysiology. From Cell to Bedside*, D.P. Zipes, J. Jalive eds., Saunders Co., Philadelphia, PA USA, 2004, p. 181.